D2

N79-24003

MODELING OF THE GEOSYNCHRONOUS PLASMA ENVIRONMENT

H. B. Garrett
Air Force Geophysics Laboratory

SUMMARY

An analytic simulation of the geosynchronous environment in terms of local time and the daily A_p index is presented. The simulation is compared with actual statistical data from approximately 50 days of ATS-5 plasma data and 50 days of ATS-6 plasma data. At low levels of activity the model adequately simulates the local time variations of the plasma parameters. At high values of geomagnetic activity, the predicted magnitudes of the plasma parameters agree with the statistical results but the effects of multiple injections are evident in both the data and the simulation, biasing the local time variations.

INTRODUCTION

The geosynchronous environment is probably the harshest space environment from a spacecraft charging standpoint. As a result, the modeling of the geosynchronous plasma and of the associated potential variations is critical to a proper understanding of spacecraft charging. As this is also the region of primary communication satellite operation, it is doubly important to accurately model this region. In this paper we will discuss the efforts of the Air Force Geophysics Laboratory in defining the geosynchronous environment. The first section will present the types of models and data available from AFGL. These models will be compared and preliminary results discussed in subsequent sections.

DEFINITION OF MODELS

Philosophical Considerations

There are at least four types of magnetospheric models that are of concern to the spacecraft charging community. Briefly, the simplest (conceptually) is a statistical compendium or histogram of various parameters as a function of space and time. Such models have little theoretical input, being based on actual measurements. Consideration of basic physical principles makes possible the creation of simple analytic expressions capable of simulating the environment - the second type of model. Third, are static field models - that is, models which employ theory to predict the trajectories of charged particles

in static magnetospheric electric and magnetic fields. Finally, the most complete models from a theoretical standpoint are full, 3-dimensional time-dependent models capable of accounting for real time variations in the plasma environment. Considering the level of our current efforts in spacecraft charging, we will limit ourselves to the first two types of models - the latter two models are much too detailed for our present needs (see Garrett, 1978, for a review of current models in each of these categories).

Statistical Model

Statistical models, as defined here, are compendiums or histograms of various plasma parameters based on actual data. Basic examples of this type of model are the distribution functions of Chan et al. (1977) who generated an "average" spectrum in terms of energy and differential number flux for various magnetospheric and solar wind regions. Likewise, Su and Konradi (1977) have averaged a year of ATS-5 geosynchronous data to obtain average particle distribution functions and other statistical parameters. Although we have taken a somewhat similar course at AFGL, we have limited our analysis to the first four integral moments (c f., DeForest and McIlwain, 1971) of the distribution function.

The 4 moments are defined as follows:

$$\langle N_i \rangle = 4\pi \int_0^\infty (V^0)\, f_i\, V^2\, dV = n_i \tag{1}$$

$$\langle NF_i \rangle = \int_0^\infty (V^1)\, f_i\, V^2\, dV = \frac{n_i}{2} \left(\frac{2kT_i}{\pi m_i}\right)^{\frac{1}{2}} \tag{2}$$

$$\langle P_i \rangle = 4\pi\, (1/3\, m_i) \int_0^\infty (V^2)\, f_i\, V^2\, dV = n_i kT_i \tag{3}$$

$$\langle EF_i \rangle = (\tfrac{1}{2} m_i) \int_0^\infty (V^3)\, f_i\, V^2\, dV = \frac{m_i n_i}{2} \left(\frac{2kT_i}{\pi m_i}\right)^{3/2} \tag{4}$$

where

$\langle N_i \rangle$ = number density for species i (number/cm^3)

$\langle NF_i \rangle$ = number flux for species i (number/cm^{2}sec-sr)

$\langle P_i \rangle$ = pressure for species i (dynes/cm^2)

$\langle EF_i \rangle$ = energy flux for species i (ergs/cm^{2}sec-sr)

The integral results on the right are for a Maxwell-Boltzmann distribution:

$$f_i\,(V) = n_i \left(\frac{m_i}{2\pi\, kT_i}\right)^{3/2} e^{\,-mV_i^2/2kT_i} \tag{5}$$

where n_i = number density of species i

m_i = mass of species i

T_i = temperature of species i

V_i = velocity of species i

K = Boltzmann constant

$f_{...}$ = distribution in sec^3/km^6

The description of the plasma in terms of these quantities is quite useful as not only are they physically meaningful in their own right, but they can be used to derive a Maxwellian or 2-Maxwellian distribution of the environment (see Garrett and DeForest, 1978).

Su and Konradi (1977) have compiled statistics on the 4 moments for ATS-5 during 1970. Their data consist of 10 minute values for the distribution functions derived from scanning ATS-5 spectrograms. We have undertaken a similar study of approximately 50 days of ATS-5 data from 1969 and 1970 and 45 days of ATS-6 data from 1974 and 1976 (Johnson et al., 1978). In our study the original digital data were integrated to give the 4 moments of the distribution function for each satellite. The ATS-6 data were corrected for satellite potential and return currents (the ATS-5 satellite spectra begin at 50 ev precluding a correction except in extreme cases like eclipses). The 4 moments were combined to give 10 minute averages (note: the 4 moments can be properly averaged in a physical and mathematical sense, the temperature cannot). For ATS-5 we have the detector components both parallel and perpendicular to the satellite spin axis, for ATS-6 we have only the component parallel to the earth's spin axis. The tapes were then merged with geophysical and ephemeris data (Garrett et al., 1978).

The tapes were and are being analyzed by a variety of techniques. In response to a desire on the part of the spacecraft charging community, we have, as a first step, compiled tables of the characteristics of the electron and ion currents and temperatures. The occurrence frequencies (note: the ATS-6 data are still being reviewed and may be subject to revision) for these parameters are plotted in figure 1. Several features are apparent in this figure which will be discussed in detail later.

An important point in the derivation of figure 1 that must be considered is the estimation of the plasma temperature from the 4 moments of the distribution function. A single temperature cannot be defined if the plasma is not Maxwellian or in the case the plasma consists of two or more Maxwellian components - circumstances which are the norm at geosynchronous orbit. As a test of this effect, we have defined two "temperatures:"

$$T\ (AVG) = \frac{\langle P \rangle}{\langle N \rangle} \qquad (6)$$

$$T\ (RMS) = \frac{\langle EF \rangle}{2\ \langle NF \rangle} \tag{7}$$

These temperatures will be equal and have meaning as temperatures <u>if and only if</u> the plasma is a Maxwellian plasma (i.e., representable by equation 5). The marked difference between T(AVG) and T(RMS) in figure 1 is a direct result of the absence of a Maxwellian plasma at geosynchronous orbit.

If the plasma is considered to consist of 2 Maxwellian components, then we can define two temperatures and two densities as follows for species i:

$$f_{2i}(V_i) = n_{1i}\left(\frac{m_i}{2\pi kT_{1i}}\right)^{3/2} e^{-m_i V_i^2/2kT_{1i}} + n_{2i}\left(\frac{m_i}{2\pi kT_{2i}}\right)^{3/2} e^{-m_i V_i^2/2kT_{2i}} \tag{8}$$

n_{1i}, T_{1i}, n_{2i}, and T_{2i} can be derived directly from equations 1 through 4. T(AVG) and T(RMS) can be expressed in terms of these quantities:

$$T\ (AVG) = k\ \frac{n_1T_1 + n_2T_2}{n_1 + n_2} \tag{9}$$

$$T\ (RMS) = k\ \frac{n_1T_1^{3/2} + n_2T_2^{3/2}}{n_1T_1^{\frac{1}{2}} + n_2T_2^{\frac{1}{2}}} \tag{10}$$

For typical values we find:

<u>For Electrons</u>	<u>For Ions</u>
$n_1 = 1/cm^3$	$n_1 = 1/cm^3$
$T_1 = 500$ eV	$T_1 = 100$ eV
$n_2 = 0.2/cm^3$	$n_2 = 1/cm^3$
$T_2 = 6000$ eV	$T_2 = 9000$ eV
$T(AVG) \simeq 1400$ eV	$T(AVG) \simeq 4550$ eV
$T(RMS) \simeq 2750$ eV	$T(RMS) \simeq 8150$ eV

These values are very close to the median values for ATS-5 shown in figure 1 and, we believe, readily explain the differences between T(AVG) and T(RMS). It is also important to note that T_1 and T_2 are not necessarily valid temperatures. They are the result of a definite fitting process - their primary use being as scaling parameters in obtaining a 2-Maxwellian fit to the distribution function. A common problem is that when the plasma is close to Maxwellian, one of the temperatures will be unrealistically large even though the fitted distribution is quite close to the actual one.

Analytic Simulation Model

In the previous section we outlined the steps involved in deriving our statistical data base and indicated some of the problems we encountered in attempting to derive "temperatures." In this section we discuss a straightforward application of the 4 moments. Briefly, a major deficiency in the statistical model of the geosynchronous orbit is that it only gives average values and ranges for given parameters, no attempt being made to preserve the simultaneous time variations in different parameters (i.e., if A is large, how do we know if B is large or small?) In order to maintain the correlated variations in different parameters, we have made use of linear regression techniques. Three hour averages of the 4 moments of the electron and ion distribution functions for 10 carefully selected days* of ATS-5 data (see Table 1) were fit by linear regression techniques to an equation varying linearly in the geomagnetic index A_p and diurnally and semidiurnally in local time LT:

$$M(LT, A_p) = (a_o + a_1 A_p)\left\{b_o + b_1 \cos\left[\frac{\pi}{12}(LT + t_1)\right] + b_2 \cos\left[\frac{\pi}{6}(LT + t_2)\right]\right\}$$

where $M(LT, A_p)$ = predicted value of the moment M at local time LT and for activity level $A_p = \frac{\sum a_p}{8}$ (i.e., daily average of a_p)

$a_o, a_1, b_o, b_1, b_2, t_1, t_2$ = coefficiencts determined by the regression (see Table 1).

To use the model, one provides A_p and local time. The model then returns the 4 moments for the electrons and ion in the units given in Table 1. The reader is referred to Garrett (1977) for a detailed discussion of the uses and

* The days were carefully selected to correspond to periods when plasma was injected while the satellite was at midnight - periods when maximum spacecraft charging is believed to take place.

applications of the model and problems associated with it. Only a cursory description will be given here.

The analytic model has been found to adequately simulate variations in the geosynchronous environment following substorm injection when a satellite is at local midnight for A_p values of ~ 4 to ~ 48 (i.e., low to moderately high activity). Above ~ 48, the model properly simulates the environment but is biased toward the plasma parameters on the particular days of high activity that were studied, not average conditions. The parameters returned by the model show the peak in charging to shift from near midnight (as expected) to near noon for high levels of activity. This was traced to the actual data for which the plasma parameters clearly peak near noon for high activity (i.e. days 348, 1970; 217 and 223, 1972). As we were careful to select only days for which injections began when the ATS-5 satellite was near midnight, this may well be a common feature of the plasma conditions associated with high activity.

MODELING RESULTS

Figure 1 presented the results which form the basis of the AFGL Environmental Specification. Figure 2 is a plot of the average local time variations of T(AVG), T(RMS), and current for ATS-5 and ATS-6. Error bars have not been indicated but they are roughly 50% of the average value. Also shown are estimates of T(AVG), T(RMS), and current for an A_p value of 15 (or average geomagnetic activity) as derived from the AFGL simulation model. For ATS-5 the results for the statistical model and the simulation model are in excellent agreement confirming that the simulation adequately predicts average conditions.

Figure 3 indicates typical (A_p = 15) and active (A_p = 207) conditions as predicted by the simulation model (the average energy is the ratio of the energy density to number density and is equal to 3/2 T(AVG)). The results are in good agreement with DeForest and McIlwain (1971) for "typical" activity levels. Figure 4 gives the results for n_1, T_1, n_2, and T_2. Note in all cases that there is an approximately X10 change in the 4 moments for the electrons and X4 for the ions with geomagnetic activity (also, the current as current density is directly proportional to number flux), but little in energy (or temperature). This observation is also born out by the statistical model (see Garrett, et al. 1978), there being, at most, a doubling of temperature.

Although the differences between ATS-5 and ATS-6 as presented in figures 1 and 2 are likely due to the near-doubling in geomagnetic activity between the ATS-5 and ATS-6 data, the foregoing observations and differences preclude an unambiguous explanation at this time. Interestingly, there is significant qualitative agreement as to the local time variation between ATS-5 and ATS-6. T(RMS), for example, peaks near 1800 for electrons and ions while the current peaks near midnight. T(AVG) peaks near 2100 for the ions (the case is not clear for the electrons). Considering the varied data sources from which the results came, this agreement is quite surprising and deserves further analysis.

CONCLUSIONS

The Air Force Geophysics Laboratory has developed two simple models of the geosynchronous plasma environment. These models were specifically developed in response to the needs of the spacecraft charging community. In summary, a detailed model (i.e., the histograms and average values versus local time) was developed based on ATS-5 and ATS-6 data. Although this model provides information on the ranges of parameters, it does not simulate actual plasma changes in time. An analytic simulation model expressible in a particularly compact form was developed in response to this latter need. The two models were shown to be consistent for average conditions. The simulation is known to predict maximum spacecraft potentials near noon for high levels of geomagnetic activity as it is deliberately biased toward injection events beginning when the satellite is near midnight. Even so, it adequately predicts geosynchronous plasma variations under a variety of conditions.

A final point is the importance of the observation that T(AVG) ≠ T(RMS) most of the time. This means that only rarely (apparently primarily at midnight) is the low energy plasma representable by a Maxwellian distribution and, hence, a temperature in the classical sense of the word. Errors as great as a factor of 3 are common between T(AVG) and T(RMS). It is, therefore, strongly recommended that a 2-Maxwellian distribution be used where possible as a minimal representation of the plasma. This distribution is readily derived by a simple algebraic expression from the 4 moments of the distribution function (see Garrett, 1977). All data and computer programs are available from AFGL.

REFERENCES

1. Chan, K. W., D. M. Sawyer, and J. J. Vette: A Model of the Near-Earth Plasma Environment and Application to the ISEE-A an -B Orbit, NSSDC/WDC-A-R&S 77-01, July 1977.

2. DeForest, S. E., and C. E. McIlwain: Plasma Clouds in the Magnetosphere, J. Geophys. Res., 76, 3587-3611, 1971.

3. Garrett, H. B.: Modeling of the Geosynchronous Orbit Plasma Environment - Part I, AFGL-TR-77-0288, 1977.

4. Garrett, H. B.: Quantitative Models of the 0 to 100 KeV Mid-Magnetospheric Particle Environment, To appear in the Proceedings of the AGU Chapman Conference on Quantitative Models of the Magnetosphere, La Jolla, CA, 18-22 September 1978, edited by W. P. Olson, 1978.

5. Garrett, H. B., G. Mullen, E. Zemba, and S. E. DeForest: ATS-5 and ATS-6 Statistical Data Atlas-Temperature, Current, and Potential at Geosynchronous Orbit, To appear as AFGL In-House Report, 1978.

6. Johnson, B., J. Quinn, and S. DeForest: Spacecraft Charging on ATS-6, Proceedings of the Symposium "The Effect of the Ionosphere on Space Systems and Communications," Washington, D.C., 1978.

TABLE 1. MULTIPLE REGRESSION COEFFICIENTS*

I	C_0	C_1	C_2	C_3	C_4	C_5	C_6	C_7	C_8	C_9
1	.38 + 02	-.42 + 02	.22 + 02	-.21 + 01	-.23 + 02	.43 + 00	-.73 - 01	-.60 - 01	-.80 - 01	.44 - 01
2	.95 + 02	-.27 + 02	.23 + 01	-.28 + 01	-.33 + 01	.21 + 00	.98 - 02	-.35 - 01	-.48 - 01	.37 - 01
3	.52 + 01	-.10 + 02	.64 + 01	.26 + 01	-.48 + 01	.13 + 00	-.28 - 01	-.33 - 01	-.20 - 01	.23 - 02
4	.77 + 02	-.45 + 01	.16 + 02	-.81 + 00	-.31 + 01	.16 + 00	-.49 - 01	.42 - 01	-.64 - 01	.24 - 01
5	.36 + 02	-.74 + 02	.50 + 02	.21 + 02	-.11 + 02	.91 + 00	-.33 - 01	-.51 + 00	-.17 + 00	-.47 - 01
6	.19 + 02	-.52 + 00	.31 + 01	-.63 - 01	-.50 + 00	.38 - 01	-.12 - 01	.15 - 01	-.18 - 01	.34 - 02
7	.47 + 02	-.68 + 02	.38 + 02	.76 + 01	-.44 + 02	.81 + 00	-.24 + 00	-.45 - 01	-.11 + 00	.50 - 01
8	.62 + 01	-.95 + 00	.14 + 01	-.13 + 00	-.30 + 00	.15 - 01	-.34 - 02	.76 - 03	-.47 - 02	.25 - 02

where:

I = 1 n_e x 100 (number/cm^3) 5 EF_e x 100 (erg/cm^2-sec-ster)

2 n_I x 100 (number/cm^3) 6 EF_I x 100 (erg/cm^2-sec-ster)

3 P_e x 10^{10} (dynes/cm^2) 7 NF_e x 10^{-6} (number/cm^2-sec-ster)

4 P_I x 10^{10} (dynes/cm^2) 8 NF_I x 10^{-6} (number/cm^2-sec-ster)

such that:

$$M_I(A_p, Lt) = C_o + C_1 \cos\left(\frac{2\pi}{24} t\right) + C_2 \sin\left(\frac{2\pi}{24} t\right) + C_3 \cos\left(\frac{4\pi}{24} t\right) + C_4 \sin\left(\frac{4\pi}{24} t\right) + C_5 A'_p + C_6 A'_p \cos\left(\frac{2\pi}{24} t\right) + C_7 A'_p \sin\left(\frac{2\pi}{24} t\right) + C_8 A'_p \cos\left(\frac{4\pi}{24} t\right) + C_9 A'_p \sin\left(\frac{4\pi}{24} t\right)$$

$t = Lt + 6.5$ $A'_p = 8 \cdot A_p$

*second number is power Lt = local time

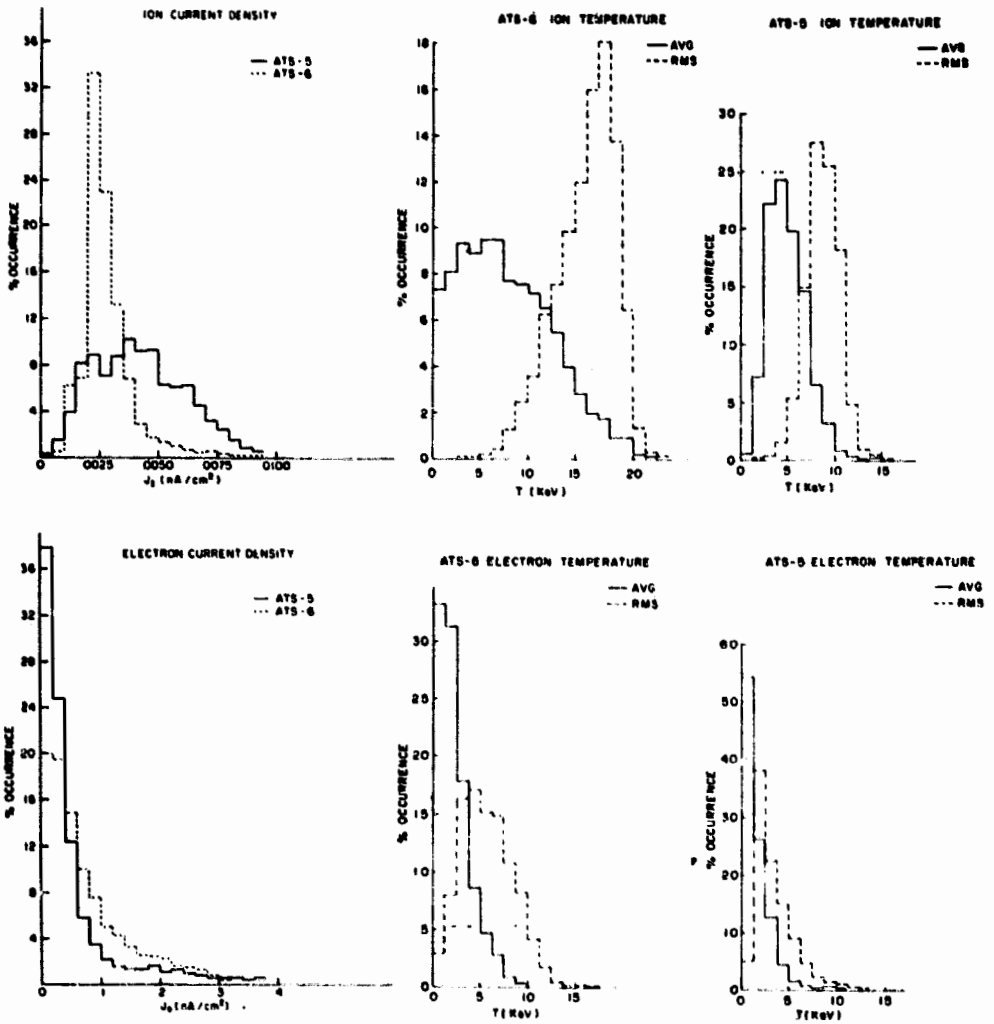

Figure 1. - Statistical occurrence frequencies of ATS-5 (1969 and 1970) and ATS-6 (1974 and 1976) electron and ion current densities, T(RMS), and T(AVG). ATS-6 values should be considered provisional.

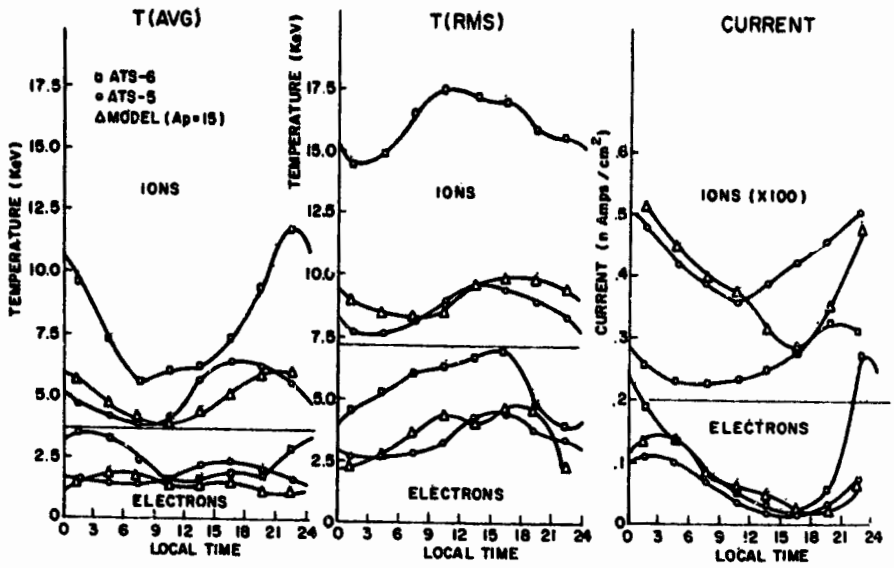

Figure 2. - Average values for current density, T(AVG) and T(RMS) for ATS-5 and ATS-6 data. Values for A_p = 15 are also plotted for simulation model. Error bars are not indicated but are approximately 50% of average value.

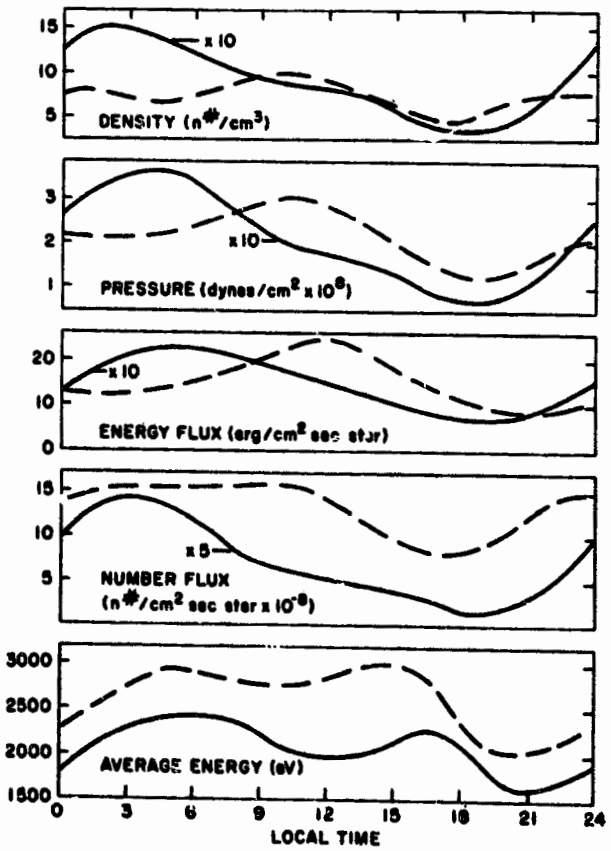

(a) Electrons.

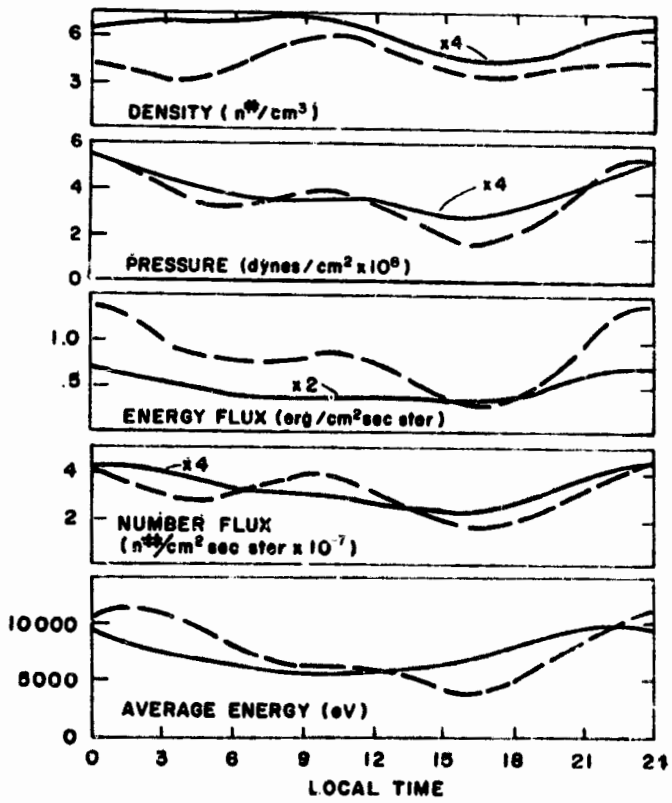

(b) Ions.

Figure 3. - Variations in 4 moments and mean energy according to AFGL simulation code for A_p = 15 (solid line) and A_p = 207 (dashed line).

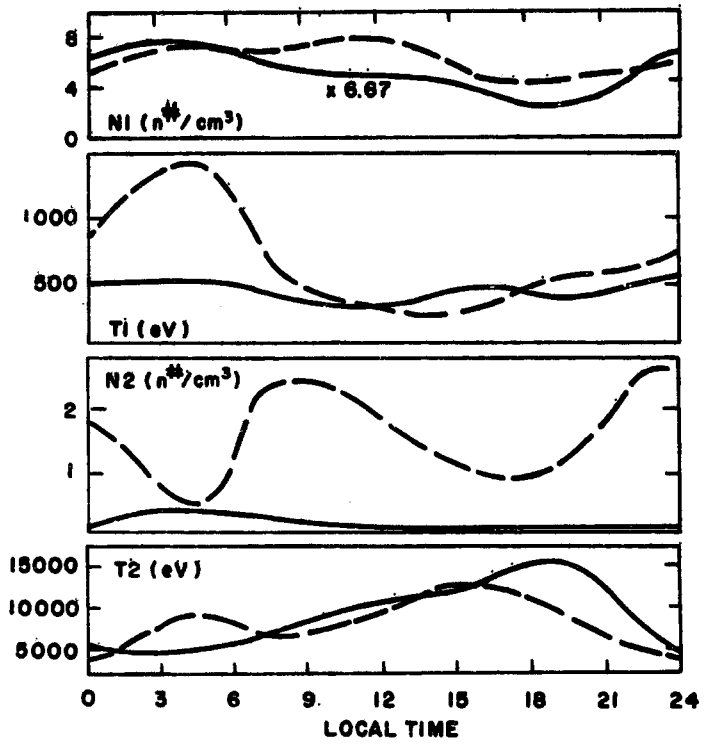

(a) Electrons.

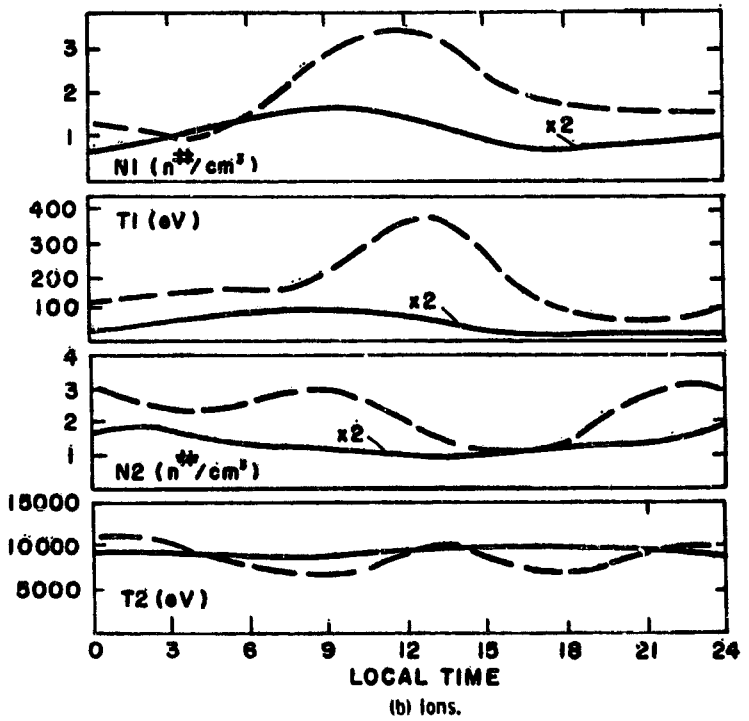

(b) Ions.

Figure 4. - Variations in N1, T1, N2, and T2 according to AFGL simulation code for A_p = 15 (solid line) and A_p = 207 (dashed line).